PERGAMON

Vision Research 41 (2001) 1791–1807

Vision Research

www.elsevier.com/locate/visres

Development of psychophysically-derived detection contours in L- and M-cone contrast space

Karen R. Dobkins [a,*], Christina M. Anderson [a], John Kelly [b,c]

[a] *Department of Psychology, 0109, University of California, San Diego, La Jolla, CA 92093, USA*
[b] *Department of Ophthalmology, Children's Hospital and Regional Medical Center, CH-61, 4800 Sand Point Way, Seattle, WA 98105-0371, USA*
[c] *Department of Ophthalmology, University of Washington, Seattle, WA 98105-0371, USA*

Received 14 September 2000; received in revised form 23 January 2001

Abstract

In order to investigate the development of color mechanisms in infants we fitted elliptical detection contours to psychophysically-derived contrast thresholds plotted in L- and M-cone contrast space. Detection ellipses were obtained for 47 infants (ages 2–5 months of age), and were compared to those of six adults tested under nearly identical conditions. The parameters of the fitted ellipses allowed us to address several aspects of color development. First, the lengths and widths were used to assess the relative development of chromatic, with respect to luminance, sensitivity. The results of these analyses revealed a sharp increase in chromatic sensitivity between 3 and 4 months of age, suggesting an accelerated development of chromatic mechanisms around this time. Second, the angles of the ellipses provided estimates of individual red/green isoluminance points. In line with previous reports, we found that isoluminance points do not vary significantly with age. Finally, our ellipse-fitting procedures were used to assess whether color sensitivity is best described by a model that assumes independence between post-receptoral chromatic and luminance mechanisms. Similar to previous results of Kelly and Chang [Kelly, J. P. & Chang, S. (2000). *Vision Research 40*, 1887–1906] obtained using steady-state visually evoked potentials, only a proportion (approximately half) of our infants exhibited detection contours that were consistent with independent mechanisms, a finding that most likely results from statistical noise in the infant data sets.

Keywords: Visual development; Chromatic; Luminance; Ellipses; Thresholds

1. Introduction

Many previous studies in adults have investigated the nature of chromatic (red/green) versus luminance mechanisms by fitting detection contours to thresholds plotted in long-wavelength-selective (L) and medium-wavelength-selective (M) cone contrast space (e.g. Noorlander, Heuts, & Koenderink, 1981; Stromeyer, Cole, & Kronauer, 1985; Poirson, Wandell, Varner, & Brainard, 1990; Chaparro, Stromeyer, Huang, Kronauer, & Eskew, 1993; Cole, Hine, & McIlhagga, 1993; Gegenfurtner & Hawken, 1995; Knoblauch & Maloney, 1996; Sankeralli & Mullen, 1996). The results from such analyses reveal several important aspects of color vision. First, the lengths and widths of the contour provide estimates of chromatic and luminance contrast thresholds. Second, the angle of the contour provides an estimate of red/green isoluminance for an individual. Third, the shape parameter reveals the degree of summation, which, depending on the angle of the contour, can indicate anything from linear summation of L- and M-cone signals to probability summation between independent chromatic (i.e. $L-M$) and luminance (i.e. $L+M$) mechanisms. The results from these adult studies typically yield elongated contours oriented significantly away from the cone-isolating axes (in either the $L+M$ or $L-M$ direction, depending upon the spatial and temporal frequency of the stimulus), with shape parameter values indicative of probability summation. Thus, such results suggest that contrast detection in adults is mediated by independent chromatic and luminance mechanisms, rather than by the total amount of contrast in L- and M-cones.

* Corresponding author. Tel.: +1-858-5345434.
E-mail address: kdobkins@ucsd.edu (K.R. Dobkins).

0042-6989/01/$ - see front matter
PII: S0042-6989(01)00070-0

In infants a single study using steady-state visually-evoked potentials (VEP) has recently examined the development of detection contours in L- and M-cone contrast space (Kelly & Chang, 2000). Using the sweep-contrast VEP technique to obtain thresholds, these investigators found that approximately 50% (seven of 13) of infant detection contours could be described by independent chromatic and luminance mechanisms, a result that was also seen in reanalyzed data from previous VEP studies (Allen, Banks, & Norcia, 1993; Morrone, Burr, & Fiorentini, 1993). Unfortunately, the relatively low number of infants in their study did not allow for systematic evaluation of variations in contour length, width, and angle as a function of age. In addition, it was shown that the steady-state VEP response was susceptible to summation and phase cancellation of underlying electrical responses, which can potentially obscure the threshold detection contour. This is because the steady-state VEP extracts a single harmonic, yet the constituent inputs can be made from any number of sinusoidal waveforms with any number of phase relationships.

In the present study we obtained psychophysically-derived contrast thresholds from infants aged 2–5 months in order to further investigate the development of detection contours in L- and M-cone contrast space. In comparison to the steady-state VEP technique, the psychophysical approach is not subject to summation and phase cancellation resulting from the VEP sources. Forty-seven infants and six adults provided thresholds along several different directions in L- and M-cone contrast space, and elliptical contours were fitted to the threshold data. For each data set we evaluated three different aspects of the fitted ellipse. First, we used the lengths and widths to estimate chromatic and luminance contrast thresholds. Although the development of chromatic and luminance sensitivity has been addressed in many previous studies (e.g. Allen et al., 1993; Morrone et al., 1993; Teller & Lindsey, 1993; Brown, Lindsey, McSweeney, & Walters, 1995; Dobkins & Teller, 1996a; Teller & Palmer, 1996; Dobkins, Lia, & Teller, 1997; Kelly, Borchert, & Teller, 1997; Crognale, Kelly, Weiss, & Teller, 1998; Dobkins, Anderson, & Lia, 1999), the present study is unique in that the ellipse-fitting procedure is expected to yield more precise estimates of chromatic (red/green) sensitivity. This is because previous studies have typically measured chromatic sensitivity using a single, nominally-isoluminant red/green stimulus, which is bound to contain luminance errors for some subjects (and thus yield overestimations of chromatic performance). By comparison, the ellipse-fitting procedure derives chromatic sensitivity based on thresholds for several stimuli, without requiring that one of these stimuli be isoluminant for an individual. Second, we used the angle of the ellipse as an estimate of each subject's personal isoluminance point. These ellipse-derived isoluminance values add to the previous literature investigating isoluminance points in infants and adults (e.g. Maurer, Lewis, Cavanagh, & Anstis, 1989; Teller & Lindsey, 1989; Brown et al., 1995; Teller, Pereverzeva, Chien, & Palmer, 2000). Finally, as was performed in the analysis by Kelly and Chang (2000), we determined, for each subject, whether the contour fit could best be described by a model assuming independent chromatic and luminance mechanisms.

2. Methods

2.1. Subjects

Infant subjects were recruited from the San Diego area. Male infants with a 25% or greater chance of dichromacy (based on family reports of colorblindness on the mother's side) were excluded from the study. In addition, female infants with a 25% or greater chance of being a carrier for dichromacy were also excluded since their red/green color vision is unpredictable (see Crone (1959) and Swanson (1991) for relevant studies in adult female carriers). All infants were born within 14 days of their due date and were reported to have uncomplicated births. A total of 63 infants participated in this study (2-month-olds, $n = 16$; 3-month-olds, $n = 13$; 4-month-olds, $n = 19$; 5-month-olds, $n = 15$). Thirteen infants (21%) failed to meet a minimum number of trials criterion (a total of at least 360 total trials). Two (3%) failed to meet a minimum performance criterion (a score of greater than 80% correct on high contrast stimuli). One infant yielded data suggestive of color-blindness, and thus his data were removed from our analyses. Thus, data from a total of 47 infants (75%) were retained (2-month-olds: $n = 12$; 3-month-olds: $n = 11$; 4-month-olds: $n = 12$; 5-month-olds: $n = 12$). On the first day of testing, the mean ages in days (x) and S.D. of our subjects were as follows: 2-month-olds: $x = 64.3$, S.D. $= 4.2$; 3-month-olds: $x = 89.4$, S.D. $= 2.9$; 4-month-olds: $x = 124$, S.D. $= 3.6$; and 5-month-olds: $x = 160.9$, S.D. $= 4.5$. For all infants testing was completed within a week.

For comparison to infant data, six adult subjects (ages 20–34) were tested under nearly identical conditions. Adult subjects had normal red–green color vision (as assessed by the Ishihara color plates) and no family history of color abnormalities. In addition, 20 adult subjects (aged 18–34) provided psychophysical red/green isoluminant points, to be used for setting an estimate of red/green isoluminance in the infant study (see below).

2.2. Apparatus

Stimuli were generated on a Nanao F2-21 monitor (21 in., 1152 × 870 pixels, 75 Hz) driven by a PowerMac 7100 computer. The 8-bit video board allowed for 256 discrete levels of luminance. The CIE coordinates for the monitor phosphors were: red (0.615, 0.342), green (0.282, 0.587), and blue (0.162, 0.069). The voltage/luminance relationship was linearized independently for each of the three guns in the display (Cowan, 1983), using a PR-650 SpectraColorimeter (Photoresearch). The PR-650 was also used for photometric measurements to standardize to V_λ isoluminance, as well as for spectroradiometric measurements to compute long-wavelength-selective (L) and medium-wavelength-selective (M) cone contrasts produced by our visual stimuli.

In order to produce the low chromatic and luminance contrasts required to span adult contrast thresholds, adult subjects were tested using specialized apparati. A second Nanao monitor (#2), which displayed a homogeneous yellow field, was placed at right angles to the main stimulus monitor (#1). A piece of plate glass (50.8 × 40.6 cm) was placed between the two monitors at a 45° diagonal, with its center 25 cm away from both monitors. Direct viewing of monitor #2 through the glass allowed approximately 87.5% transmittance of light from monitor #2 and 12.5% reflection of light from monitor #1. The mean luminances on the two monitors (19.1 and 87.0 cd/m^2 for monitors #1 and #2, respectively) produced a combined luminance of 80.6 cd/m^2, which was then attenuated to 17.5 cd/m^2 at the eye (to match infant conditions, see below) by having subjects wear glasses that contained 0.66 neutral density filters. This set-up resulted in a 97% reduction in contrast for gratings presented on monitor #1.

2.3. Stimuli

Stimuli were horizontally-oriented, moving (upwards or downwards) sinusoidal gratings, viewed binocularly from a distance of 38 cm. Note that we chose to use moving, rather than counterphase, gratings because the relatively higher thresholds for the latter (e.g. Dobkins et al., 1997) decreases the likelihood of producing high enough contrasts to capture infant thresholds (specifically for chromatic stimuli). Grating size was 15 × 15° of visual angle, presented on a background subtending 59 × 45°. The spatial frequency of the gratings was set at 0.27 cyc/deg to optimize detectability for ages 2–5 months (e.g. Atkinson, Braddick, & Moar, 1977; Banks & Salapatek, 1978). In addition, this spatial frequency is low enough to avoid luminance artifacts associated with chromatic aberration (e.g. Flitcroft, 1989; Cavanagh & Anstis, 1991). Motion was produced by phase-shifting the gratings at regular intervals in sync with the vertical refresh of the video monitor (75 Hz). The temporal frequency of the gratings was set at 4.7 Hz (phase shift = 20, speed = 15.4 deg/s), chosen because it is near the peak of the infant temporal contrast sensitivity function for chromatic and luminance stimuli (Hartmann & Banks, 1992; Dobkins & Teller, 1996b; Rasengane, Allen, & Manny, 1997; Dobkins et al., 1999). Due to the relatively small size of our stimuli, moving gratings did not elicit any noticeable tracking eye movements in our subjects.

Gratings were modulated through a yellow point (CIE $x, y = 0.478, 0.425$) at a space average luminance of 22.0 cd/m^2. Gratings were constructed using mainly the red and green phosphors on the monitor, with a small amount of blue phosphor added in phase with the red phosphor so as to yield no modulation of short-wavelength-selective (S) cones. The purpose of modulating through yellow (rather than white) was 2-fold. First, it allowed us to produce higher cone contrasts in L- and M-cones, which increased the likelihood that we would capture infant thresholds for isoluminant red/green stimuli. On our monitor, the maximum cone contrasts produced by V_λ-isoluminant stimuli were 14.4 and 36.4% for L- and M-cones, respectively. Second, stimuli modulated through yellow produced extremely low S-cone activation (approximately 0.003 units in MacLeod & Boynton 1979 chromaticity space), and thus the contribution of S cones to our threshold estimates is expected to be negligible.

2.4. L- and M-cone contrast space

The goal of these experiments was to plot thresholds in cone contrast space and fit them with detection contours (see Fig. 1). Here, the L-cone contrast of the stimulus is plotted along the abscissa (0°/180°) and the M-cone contrast of the stimulus is plotted along the ordinate (90°/270°). Positive contrasts denote cone excitations above the mean excitation level, whereas negative contrasts denote cone excitations below the mean. A yellow/black 'luminance' grating modulates the L- and M-cones equally and in spatial register with one another and is thus represented along the 45° diagonal (referred to as the 'L + M axis'). The yellow phase of the grating produces positive contrast while the black phase produces negative contrast. Since the stimuli are gratings, the thresholds are forced to be symmetric about the origin. A red/green isoluminant 'chromatic' grating modulates L-cones in spatial opposition to M-cones, and is thus represented along the L − M direction (at approximately 135°, but will depend on the subject and stimulus parameters). The L- and M-cone excitations (and contrasts) produced by our stimuli were obtained with a PR-650 SpectraColorimeter, by integrating the product of stimulus spectral output

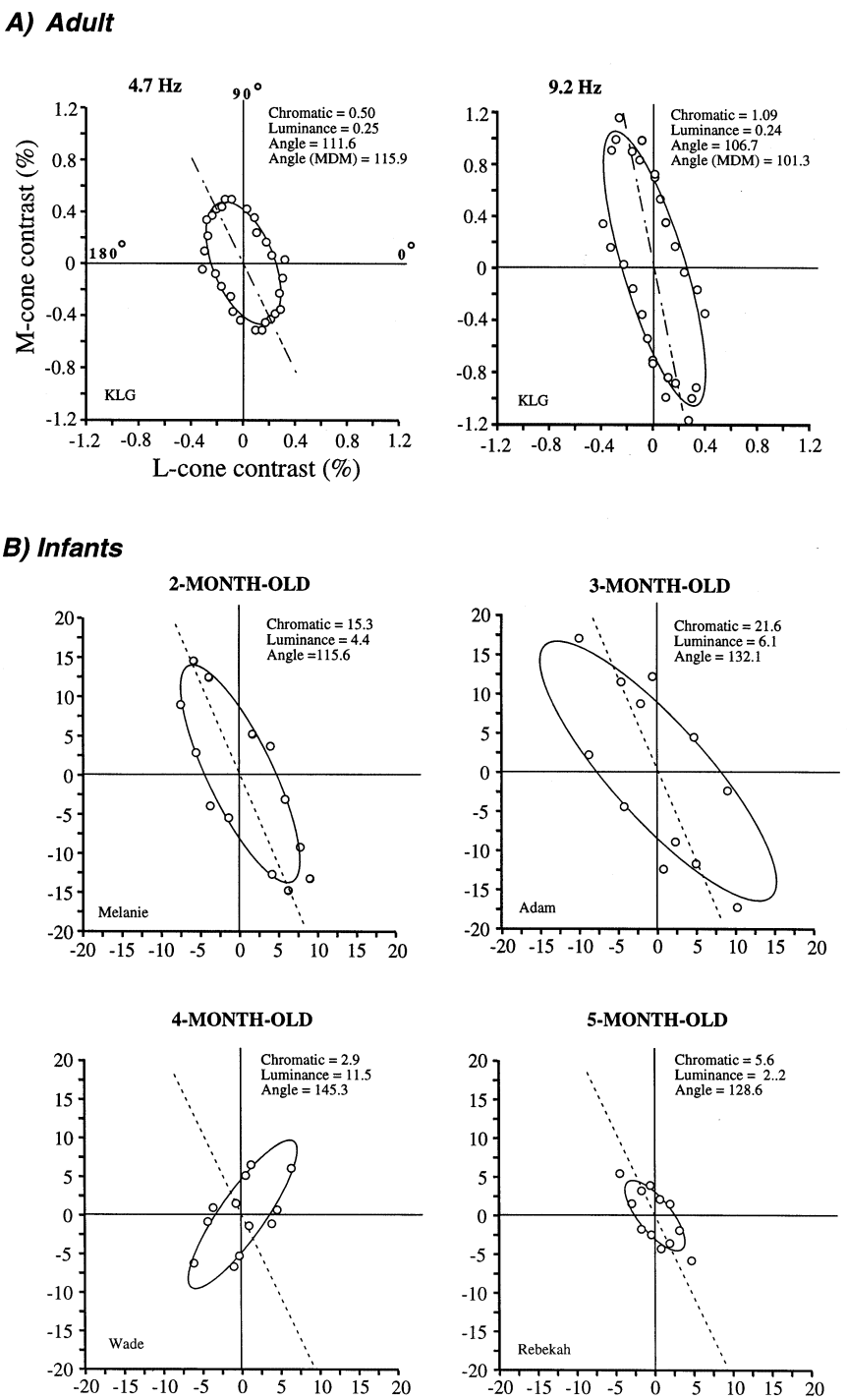

Fig. 1. Example ellipses plotted in L- and M-cone contrast space. (A) Data from an adult subject tested at 4.7 Hz (left panel) and 9.2 Hz (right panel). At both temporal frequencies, the ellipse is oriented in the L − M direction, indicating higher chromatic, with respect to luminance, thresholds. The angle of the ellipse in the L − M direction represents the individual's isoluminance point. The dotted-dashed line represents the angle of the subject's isoluminance point as determined from our minimally-distinct motion (MDM) technique (see Section 2). The estimated values for chromatic threshold, luminance threshold, and isoluminance angles are provided in the insets. (Note that 0° denotes alignment with the L-cone axis, while 90° denotes alignment with the M-cone axis.) (B) Representative ellipses for individual 2-, 3-, 4- and 5-month-old infants tested at 4.7 Hz. Here, the dashed line represents the mean isoluminance point across 20 adult subjects tested with our minimally-distinct motion technique (115.2°), which was used to create a nominally-isoluminant stimulus for infants. Three of the four infants yielded an ellipse oriented along the L − M direction, indicating higher chromatic, with respect to luminance, thresholds. Conversely, data from the 4-month-old yielded an ellipse oriented in the L + M direction, indicating a relatively higher luminance threshold.

(readings taken in 4 nm intervals from 380 to 780 nm) with the Stockman, MacLeod, and Johnson (1993) L- and M-cone fundamentals. Because cone fundamentals are expected to differ somewhat across individuals (based on differences across subjects in λ_{max}, photopigment optical density, as well as lens and macular pigment), we expect some error in cone contrasts derived from a standard set of cone fundamentals for all subjects (see Bieber, Kraft, & Werner (1998)).

Each infant subject was tested at six different angles in L- and M-cone space. Two of the six stimuli included a yellow/black (luminance) and a nominally-isoluminant red/green (chromatic) stimulus. The latter was set for all infants using the mean isoluminance point determined from 20 adult subjects tested with a 'minimally-distinct motion' technique (e.g. Dobkins & Teller, 1996a). Specifically, adult subjects adjusted the luminance contrast in a moving red/green grating (0.27 cyc/deg, 4.7 Hz) until the percept of motion was least salient. For each subject, isoluminance was determined from the mean of twenty trials. Across our adult subjects, the mean isoluminance value was oriented at 115.2° in L- and M-cone space (Fig. 1b, dashed lines). Based on results from previous studies, we expect this adult value to be a good estimate of isoluminance for infants (Maurer et al., 1989; Teller & Lindsey, 1989; Morrone et al., 1993; Bieber, Volbrecht, & Werner, 1995; Brown et al., 1995; Chien, Teller, & Palmer, 2000; Teller et al., 2000). However, owing to differences in isoluminance across subjects, we know that this stimulus cannot be isoluminant for all infant subjects. Fortunately, our analyses do not rely on this value being precise, since isoluminance is obtained for each individual using the contour fit to all six data points (see below). The four other stimuli were various combinations of luminance and chromatic contrast. Although it would have been optimal to use constant angular spacing of the six stimuli (i.e. spaced in 30° intervals), the spacing of our stimuli varied somewhat across subjects. This is due to the fact that these stimuli were originally designed for a different study (Anderson & Dobkins, 1999), which did not require tight control of this parameter. On average, the spacing was 24.2°.

2.5. Psychophysical paradigm

Infant contrast thresholds were determined using the forced-choice preferential looking (FPL) technique (Teller, 1979) with the method of constant stimuli, as described in detail previously (see Dobkins & Teller (1996a,b)). Briefly, an adult experimenter held the infant 38 cm away from the front of the stimulus monitor in the view of a video camera aimed at the infant's face. On each trial, the grating stimulus appeared on the left or right side of the video monitor (centered at 15° eccentricity), and the experimenter used cues such as the infant's head turning and gazing behavior to judge the left versus right location of the stimulus. Computer beeps provided feedback to the adult experimenter. Stimuli were presented in a contrast-ramped fashion, with stimulus contrast increasing (in a sinusoidal fashion) from zero to the specified contrast over the course of one motion cycle. For each of the six stimuli, five different contrast levels were presented.

Our goal was to obtain a minimum of 360 trials from each infant, such that there were at least 60 trials obtained for each of the six psychometric functions. The total number of trials obtained per psychometric function ranged from 60 to 120, with an average of 71, 78, 81 and 62 for 2-, 3-, 4- and 5-month-olds, respectively (S.D.s = 9.6, 13, 19 and 7.8, respectively).

2.6. Adult testing

Contrast thresholds in adults were obtained by standard forced-choice psychophysical techniques with feedback, under conditions that were nearly identical to those of infants (gratings = 0.27 cyc/deg, modulated through yellow, CIE $x, y = 0.439, 0.463$, at a space average luminance of 17.5 cd/m^2). On each trial, the stimulus appeared on the left or right side of the display and the subject reported its location with a key press. As for infants, eye position in our adult subjects was unrestricted and stimuli remained present on the screen until a decision was made.

Each adult subject was tested at 14 different angles in L- and M-cone contrast space, one of which included her own red/green isoluminance point determined from the minimally-distinct motion technique (see above). Here, the average spacing was 12.0° (optimal spacing = 12.86 deg). Adults were tested at two temporal frequencies; one which was the same as that employed for infants (i.e. 4.7 Hz) and one which was double that temporal frequency (i.e. 9.4 Hz). Our reason for testing adults at this higher temporal frequency was to see if infant ellipses at 4.7 Hz resemble adult ellipses at 9.2 Hz. This could occur if 4.7 Hz is a relatively high temporal frequency for infants (e.g. see Dobkins et al. 1997, 1999). For adults, the total number of trials obtained per psychometric function was 120.

2.7. Data analysis

2.7.1. Contour fitting

Contrast thresholds were derived from Weibull functions fitted to the data for each stimulus condition (see Dobkins et al. 1999 for details of psychometric function fittings in infants and adults). Thresholds were plotted in L- and M-cone contrast space, and detection contours were fitted to the data. Details of the contour-fitting procedure and its underlying theory have been described previously (Kelly & Chang, 2000 and see

Noorlander, Heuts, & Koenderink, 1981; Stromeyer et al., 1985; Poirson et al., 1990; Cole et al., 1993; Knoblauch & Maloney, 1996; Sankeralli & Mullen, 1996). Briefly, contours were transformed into a single polar coordinate system, where each color direction i has an L-cone and M-cone threshold (L_c, M_c) of magnitude r_i with a set polar angle ϕ:

$$r_i\phi = \sqrt{(L_c^2 + M_c^2)}. \quad (1)$$

The basic form of the contour is:

$$x = a\cos(\theta)^e \qquad y = b\sin(\theta)^e \quad \{0 \le \theta \le 2\pi\}, \quad (2)$$

where a and b are the length and width, respectively, e defines the shape of the contour, and θ is the polar direction in color space.

The contour is then rotated by:

$$x' = x^*\cos(\rho) + y^*\sin(\rho)$$
$$y' = -x^*\sin(\rho) + y^*\cos(\rho) \quad \{0 \le \rho \le 2\Pi\}, \quad (3)$$

where ρ defines the angular rotation of the contour (with 0° reflecting alignment with the L-cone axis, and 90° reflecting alignment with the M-cone axis, see Fig. 1). The predicted threshold, C_i, is the magnitude of the contour at ϕ. A reiterative program then minimizes the sum of squares of the log difference between the predicted contour point $C_i\phi$ and the threshold value $r_i\phi$. In the Kelly & Chang, 2000 study, contours were fit with four free parameters: a (length), b (width), e (shape), and ρ (angle). However, for the present study, detection contours were constrained to be ellipses (i.e. e was fixed at 1.0 in Eq. (2)). The reason for doing so was based on the finding that, statistically, ellipses fit the data as well as, if not better than, the more complex contour (75% of the adult data sets in the present study, and 62% of data sets in Kelly & Chang, 2000). In addition, by reducing the number of free parameters, there are fewer chances to arbitrarily fit noisy data points.

2.7.2. Luminance and chromatic contrast thresholds and isoluminance angles

In order to obtain estimates of chromatic and luminance thresholds, as well as individual isoluminance points, we evaluated the fit of each subject's data set with two main models. The first (and simplest) model assumes that thresholds are determined by the total contrast produced in L- and M-cones (specifically, by a root-mean-squared sum of L- and M-cone contrasts). The detection contour is a circle, in which the only free parameter is its diameter (i.e. length (a) and width (b) are set to be the same). We refer to this model as the *circle model*, even though a circle is technically a subset of the ellipse category. The second model, which we refer to as the *standard ellipse model*, has three free parameters (i.e. length (a), width (b), and angle (ρ). The fit of the two models was evaluated statistically by an F-ratio, which compares the amount of residual error between the models. For each subject's data set, we accepted the standard ellipse model over the circle model when the residual error in the former was significantly less than that in the latter (see Kelly & Chang, 2000 for details).

For subjects whose data were best described by the standard ellipse model, with the ellipse oriented in the L − M direction, the angle of the major axis was taken as the subject's isoluminance point, the length was taken as the subject's chromatic contrast threshold and the width as the luminance contrast threshold. Conversely, if the ellipse was oriented in the L + M direction, the length was taken as the luminance contrast threshold, and the width was taken as the chromatic contrast threshold. For subjects who were best described by the circle model, the diameter of the circle determined both the chromatic and luminance threshold, however, no isoluminance angle could be obtained for such data sets.

2.7.3. Independence of chromatic and luminance mechanisms

In order to investigate the existence of independent chromatic and luminance mechanisms, we compared the fit of our standard ellipse model to that of a third model, which assumes that thresholds are determined by an unequal sum of L- and M-cone contrasts. This detection contour is an ellipse that is uniquely oriented along either the L- or M-cone isolating axis. We refer to this as the *fixed-angle ellipse model*, which has two free parameters (i.e. length (a) and width (b)), while ρ is fixed to be aligned within $\pm 4°$ of one of the two cone axes (to allow for small differences in cone fundamentals across subjects, see Kelly and Chang (2000)). In essence, the fixed-angle ellipse model is a more general form of the circle model (which also assumes cone summation), since the fixed-angle ellipse can readily be conformed into a circle when the L- and M-cone axes are rescaled (Poirson et al., 1990).

In contrast to the fixed-angle ellipse model, which assumes that detection is limited by the sum of cone contrasts, a contour generated by the standard ellipse model that is oriented away (i.e. greater than $\pm 4°$) from the cone isolating axes is suggestive of independent chromatic and luminance mechanisms. For each subject's data, the fitted contour was accepted as consistent with independent mechanisms when the residual error in the standard ellipse model was significantly less than that from the fixed-angle ellipse (i.e. cone summation) model.

3. Results

3.1. Example ellipses

Standard ellipses fitted to the data from one adult subject are shown in Fig. 1a, for both the 4.7 Hz (left panel) and 9.2 Hz (right panel) conditions. Each ellipse was derived from 28 values (i.e. based on 14 thresholds, which were then symmetrically reflected around the origin). The length of the contour along the L − M direction provides an estimate of the subject's chromatic (red/green) threshold, while the width along the L + M direction provides a luminance threshold estimate. At both temporal frequencies, the ellipses were oriented along the L − M direction, indicating higher chromatic, with respect to luminance, thresholds. The angle of the ellipse (with 0° denoting alignment with the L-cone isolating axis and 90° denoting alignment with the M-cone isolating axis) represents the individual's isoluminance point as determined from the contour-fitting procedure. These values were 111.6° and 106.7° at 4.7 and 9.2 Hz, respectively. For comparison, the dotted-dashed line represents the angle of the subject's isoluminance point as determined from our minimally-distinct motion technique (see Section 2). Here, the values were 115.9° and 101.3° at 4.7 and 9.2 Hz, respectively. The close correspondence between the two measures indicates that the angle of the ellipse provides an adequate estimate of the individual's isoluminance point as determined in a more direct fashion. The estimated values for chromatic threshold, luminance threshold, and isoluminance angles are provided in the inset of each graph.

Representative ellipses for 2-, 3-, 4- and 5-month-old infants tested at 4.7 Hz are shown in Fig. 1b. For infants, each ellipse is derived from 12 values (i.e. based on six thresholds). Here, the dashed line at 115.2° represents the mean isoluminance point across 20 adult subjects tested with the minimally-distinct motion technique, which was used to create a nominally-isoluminant stimulus for infants. Our analyses do not rely on this nominal isoluminance point being precise, since individual isoluminance was obtained separately for each subject using the contour fit to all six threshold values. It is also important to point out that, because some infant ellipses are expected to be oriented away from the nominal isoluminance point, the ellipse-fitting procedure provides a more accurate estimate of chromatic contrast threshold than that which would have been obtained had we simply used the threshold for the nominally-isoluminant stimulus. For example, while the alignment with nominal isoluminance was very close for the 2-month-old in this example (individual isoluminance = 115.6°), it was quite disparate for the 3-month-old (individual isoluminance = 132.1°).

With regard to chromatic and luminance thresholds, three of the four infants (the 2-, 3- and 5-month-old) yielded an ellipse oriented along the L − M direction, indicating higher chromatic, with respect to luminance, thresholds. Conversely, data from the 4-month-old yielded an ellipse oriented in the L + M direction, indicating a relatively higher luminance threshold. This reversed pattern was fairly representative of our 4-month-old subjects, as supported by the group ellipses presented in Fig. 2.

3.2. Group data

Data from all subjects are shown in Fig. 2a (adults) and b (infants). In addition, the best fitting parameters (a, b and ρ) for each individual's standard ellipse fit are provided in Table 1. As described in the Methods, the contour fit to the data points was determined by one of two models; one that allowed the fitted contour to have different values for length (a) and width (b) and allowed the angle (ρ) to vary freely (i.e. the standard ellipse model) and one where a and b were constrained to be the same (i.e. the circle model). We accepted the circle model (which is the simplest in having only one free parameter) if it could account for the variance as well as the standard ellipse model (which is more complex, with three free parameters). Our purpose in pitting these two models against one another was to ensure that we were not forcing an oriented ellipse in cases where a circle provided a simpler description of the data. Individuals who were best fit by the circle model are plotted separately (upper/right inset in each graph) from those best fit by the standard ellipse model, so that the contours for the latter would not be obscured. In adults, the standard ellipse model proved superior in all but one subject, when tested at 4.7 Hz. For infants, the standard ellipse model proved superior in the majority (77%) of cases: 100% (12/12) of 2-month-olds, 91% (10/11) of 3-month-olds, 50% (6/12) of 4-month-olds and 66.7% (8/12) of 5-month-olds.

There are several things to note in these group ellipses. First, as expected, the overall sizes of the ellipses decreased with age. Second, the angle of the ellipses varied across individuals at each age. Third, the vast majority of ellipses in 2-, 3-, 5-month-olds and adults were oriented in the L − M direction, indicating higher chromatic, with respect to luminance, thresholds. For 4-month-olds, however, we found a somewhat surprising reversal; out of six infants that were best fit by the standard ellipse model, five were clearly orientated in the L + M direction. In addition, the other half (6/12) of our 4-month-olds were best fit by the circle model, suggesting that this age may reflect a time of cross-over between superior chromatic versus luminance sensitivity. Finally, infant ellipses more closely resembled adult ellipses obtained at 4.7 Hz than at 9.2 Hz. Specifically,

for adults, the mean chromatic/luminance threshold ratio was 1.49 and 3.30 for 4.7 and 9.2 Hz, respectively. For infants, the mean threshold ratio across all infants was 1.46, which was statistically indistinguishable from adults at 4.7 Hz ($t_{(df=46)} = 0.17$, $P = NS$), yet significantly different from adults tested at 9.2 Hz ($t_{(df=46)} = 7.23$, $P < 0.005$). Such findings thus reject the possibility that data from infants tested at 4.7 Hz might resemble that of adults tested at a higher temporal frequency.

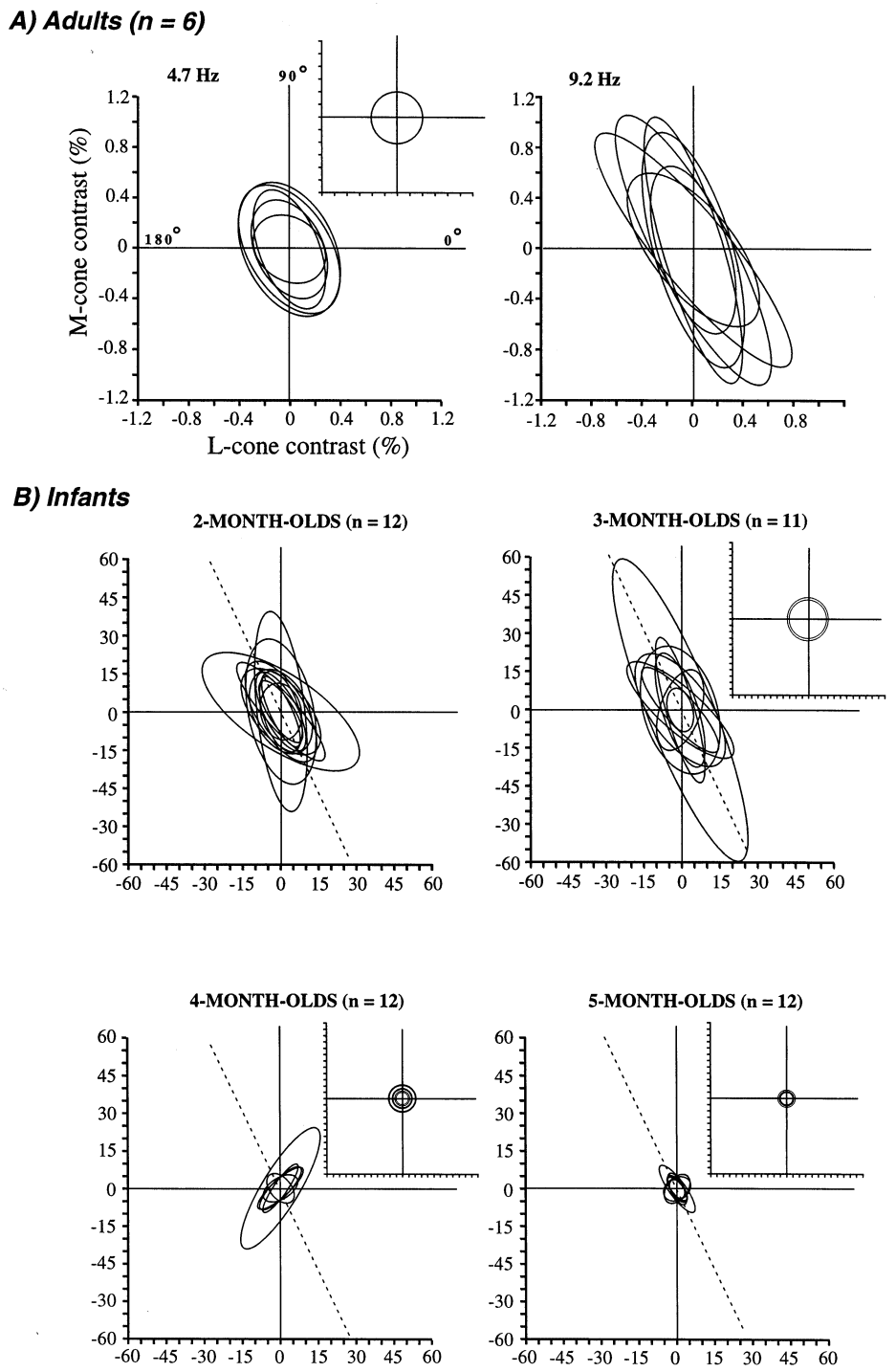

Fig. 2. Group ellipses. (A) Adults tested at 4.7 Hz (left panel) and 9.2 Hz (right panel) ($n = 6$). (B) Data from 2-month-olds ($n = 12$), 3-month-olds ($n = 11$), 4-month-olds ($n = 12$) and 5-month-olds ($n = 12$). As for Fig. 1b, the dashed line represents the mean adult isoluminance point (115.2°). (No dashed lines are presented for adults, since each adult was tested with a red/green stimulus that was individually set to isoluminance.) The best fitting parameters (a, b and ρ) for each individual's standard ellipse fit are provided in Table 1. See text for details.

Table 1
Summary of curve fitting parameters[a]

	Standard ellipse model				Cone summation model				Accept independent chromatic and luminance mechanisms?
	Length (a)	Width (b)	Angle (ρ)	MS error	Length (a)	Width (b)	Angle (ρ)	MS error	
2-Months									
S1	*16.3*	*6.8*	*107.5*	*0.030*	*17.2*	*6.5*	*94.0*	*0.032*	*No*
S2	13.6	5.1	122.8	0.011	11.0	6.8	94.0	0.037	Yes, $P = 0.001$
S3	*11.0*	*8.0*	*101.6*	*0.007*	*11.1*	*8.2*	*94.0*	*0.007*	*No*
S4	36.1	14.6	146.6	0.009	19.8	16.6	94.0	0.014	Yes, $P < 0.05$
S5	*28.6*	*12.7*	*101.8*	*0.042*	*30.7*	*13.0*	*94.0*	*0.038*	*No*
S6	*17.4*	*11.3*	*116.0*	*0.007*	*16.0*	*11.9*	*94.0*	*0.009*	*No*
S7	22.0	9.7	121.2	0.010	19.0	10.2	94.0	0.020	Yes, $P < 0.01$
S8	*39.3*	*9.8*	*96.4*	*0.011*	*43.1*	*9.8*	*86.0*	*0.020*	*No*
S9	16.5	6.8	118.0	0.009	14.5	9.4	94.0	0.021	Yes, $P < 0.005$
S10	15.3	4.4	115.6	0.002	13.3	5.4	94.0	0.028	Yes, $P < 0.001$
S11	*24.9*	*6.4*	*131.7*	*0.032*	*13.3*	*7.5*	*94.0*	*0.043*	*No*
S12	20.1	10.8	131.4	0.006	15.0	12.9	94.0	0.017	Yes, $P < 0.005$
3-Months									
S1	21.6	6.1	132.1	0.007	12.6	8.1	94.0	0.022	Yes, $P = 0.001$
S2	***11.1***	***10.4***	***0.7***	***0.020***	10.4	9.2	94.0	0.018	***No***
S3	25.7	12.1	125.7	0.013	19.6	13.7	94.0	0.020	Yes, $P < 0.05$
S4	25.9	14.2	106.8	0.000	27.3	13.4	94.0	0.002	Yes, $P < 0.001$
S5	23.7	6.6	108.2	0.007	18.8	8.1	94.0	0.017	Yes, $P < 0.005$
S6	***14.5***	***10.4***	***161.7***	***0.021***	14.0	10.7	176.0	0.020	***No***
S7	29.2	6.1	106.0	0.009	29.4	6.9	94.0	0.031	Yes, $P = 0.001$
S8	8.1	5.0	105.9	0.003	8.2	4.9	94.0	0.004	No
S9	63.9	13.0	112.0	0.026	49.1	11.8	94.0	0.046	Yes, $P < 0.025$
S10	*16.4*	*8.6*	*70.4*	*0.008*	*13.2*	*8.8*	*86.0*	*0.010*	*No*
S11	26.7	8.4	138.8	0.003	13.6	10.4	94.0	0.016	Yes, $P = 0.001$
4-Months									
S1	***7.9***	***7.1***	***153.1***	***0.004***	***7.8***	***7.2***	***176.0***	***0.003***	***No***
S2	11.3	3.4	46.5	0.001	5.6	5.1	4.0	0.030	Yes, $P < 0.001$
S3	7.5	4.3	32.5	0.001	6.5	5.2	4.0	0.006	Yes, $P = 0.001$
S4	***10.4***	***5.9***	***33.4***	***0.024***	***8.5***	***7.4***	***4.0***	***0.026***	***No***
S5	***4.4***	***3.7***	***73.0***	***0.002***	***4.3***	***3.7***	***86.0***	***0.002***	***No***
S6	***4.3***	***2.7***	***109.5***	***0.035***	***4.4***	***2.7***	***94.0***	***0.034***	***No***
S7	***6.3***	***4.1***	***109.1***	***0.009***	***5.8***	***4.3***	***94.0***	***0.009***	***No***
S8	27.5	7.3	58.7	0.012	15.3	11.6	86.0	0.044	Yes, $P < 0.005$
S9	6.8	4.5	129.6	0.005	5.5	5.4	176.0	0.007	Yes, $P < 0.05$
S10	***6.5***	***4.7***	***87.6***	***0.007***	***6.5***	***4.7***	***88.6***	***0.007***	***No***
S11	11.5	3.2	47.2	0.001	5.8	4.5	86.0	0.037	Yes, $P < 0.001$
S12	11.5	2.8	55.3	0.019	5.9	3.6	86.0	0.055	Yes, $P < 0.005$
5-Months									
S1	6.3	4.0	52.5	0.002	5.3	4.7	86.0	0.006	Yes, $P < 0.005$
S2	3.7	2.5	121.9	0.002	3.5	2.9	94.0	0.005	Yes, $P < 0.005$
S3	5.6	4.5	33.6	0.001	5.3	4.7	4.0	0.002	Yes, $P < 0.05$
S4	***4.4***	***3.7***	***90.5***	***0.018***	***4.4***	***3.7***	***90.4***	***0.016***	***No***
S5	***7.3***	***4.5***	***154.0***	***0.010***	***6.8***	***4.7***	***176.0***	***0.013***	***No***
S6	5.6	2.7	125.7	0.012	4.7	3.2	94.0	0.018	Yes, $P < 0.05$
S7	***5.1***	***3.7***	***159.2***	***0.020***	***5.2***	***3.6***	***176.0***	***0.019***	***No***
S8	***4.6***	***3.0***	***28.0***	***0.010***	***4.0***	***3.2***	***4.0***	***0.011***	***No***
S9	*6.1*	*2.4*	*123.3*	*0.047*	*5.0*	*2.7*	*94.0*	*0.062*	*No*
S10	*6.5*	*2.9*	*115.7*	*0.014*	*5.3*	*3.1*	*94.0*	*0.018*	*No*
S11	5.6	2.2	128.6	0.010	3.8	3.4	94.0	0.032	Yes, $P = 0.001$
S12	10.9	2.9	125.6	0.009	6.2	4.4	94.0	0.033	Yes, $P = 0.001$
Adults (4.7 Hz)									
S1	0.56	0.36	115.9	0.005	0.54	0.39	94.0	0.008	Yes, $P = 0.010$
S2	0.50	0.25	111.6	0.002	0.48	0.27	94.0	0.007	Yes, $P = 0.001$
S3	0.31	0.24	141.8	0.005	0.29	0.27	176.8	0.006	Yes, $P = 0.025$
S4	***0.39***	***0.26***	***102.6***	***0.007***	***0.31***	***0.28***	***94.0***	***0.004***	***No***
S5	0.42	0.27	116.5	0.005	0.40	0.28	94.0	0.007	Yes, $P = 0.010$
S6	0.56	0.33	120.9	0.008	0.50	0.39	94.0	0.013	Yes, $P = 0.010$

Table 1 (Continued)

	Standard ellipse model				Cone summation model				Accept independent chromatic and luminance mechanisms?
	Length (a)	Width (b)	Angle (ρ)	MS error	Length (a)	Width (b)	Angle (ρ)	MS error	
Adults (9.2 Hz)									
S1	0.96	0.31	106.7	0.003	0.94	0.34	94.0	0.011	Yes, $P<0.001$
S2	1.09	0.24	106.7	0.003	0.89	0.26	94.0	0.018	Yes, $P<0.001$
S3	0.73	0.32	128.7	0.006	0.58	0.46	94.0	0.022	Yes, $P<0.001$
S4	0.68	0.27	108.0	0.002	0.62	0.31	94.0	0.008	Yes, $P<0.001$
S5	1.19	0.31	117.8	0.002	0.89	0.39	94.0	0.026	Yes, $P<0.001$
S6	1.17	0.28	129.6	0.008	0.64	0.51	94.0	0.060	Yes, $P<0.001$

[a] Parameters for length (a), width (b), angle (ρ) and mean square (MS) error of ellipses fitted to threshold data, for two models: the standard ellipse model (angle was allowed to vary freely) and the cone summation model (i.e. 'fixed-angle ellipse model', angle constrained within $\pm 4°$ of one cone axis). The shape parameter (e) is set to 1.0 for both (see Eq. (2) in Section 2). For each subject, data were accepted as consistent with independent mechanisms only when the residual error in the standard ellipse model was significantly less than that from the cone summation model (see text). Italicized cells represent data from individuals for whom the circle model had originally been rejected, yet their data were best described by the cone summation model in this analysis. Bold subjects represent individuals presented in the example data of Fig. 1. Bold italic cells represent data from individuals who were better fit by the circle model as opposed to the standard ellipse model in our original analyses. In each of these cases, as expected, the data were also better described by the cone summation model.

3.3. Group mean cone contrast sensitivity as a function of age

In order to examine these developmental changes further, we have plotted group mean cone contrast sensitivity (sensitivity = 1/threshold) as a function of age in Fig. 3 (open circles and squares). These sensitivity values were derived from the lengths and widths of the fitted contours. For subjects with ellipses oriented along the L − M direction, the length provided a chromatic threshold while the width provided a luminance threshold. For subjects with ellipses oriented along the L + M direction, the converse is true. For subjects best fit by the circle model, the length and width parameters were necessarily equal to one another, and thus chromatic and luminance thresholds were taken to be identical.

The results of this analysis demonstrate a steeper increase in chromatic, with respect to luminance, sensitivity between 2 and 5 months of age. In particular, there is a marked increase in chromatic, but not luminance, contrast sensitivity between 3 and 4 months of age. In fact, this increase in chromatic sensitivity is so great as to create a reversal in the relative sensitivity for chromatic versus luminance contrast at 4 months. As expected based on the group ellipses presented in Fig. 2, 4-month-olds were more sensitive to chromatic than to luminance contrast, whereas all other ages (including adults) showed the opposite pattern. These results are strikingly similar to those of our previous study, which investigated the development of chromatic and luminance temporal contrast sensitivity functions in infants (Dobkins et al., 1999). For comparison, we have plotted the data from this previous study obtained from infants (3- and 4-month-olds) and adults tested at 4.2 Hz, 0.27 cyc/deg (Fig. 3, filled circles and squares, data shifted upwards to facilitate comparison). Note that these earlier data were obtained by testing infants with only two stimuli; a yellow/black (luminance) stimulus and a nominally-isoluminant red/green stimulus.

At first glance the relatively steeper increase in chromatic, with respect to luminance, sensitivity between 2 and 5 months might be viewed as evidence for faster development of chromatic, with respect to luminance,

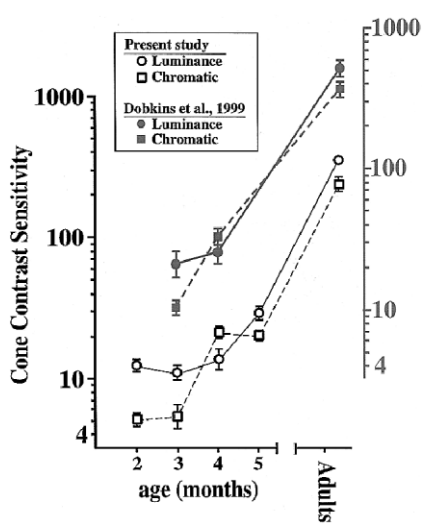

Fig. 3. Development of chromatic and luminance contrast sensitivity. Shown are the mean cone contrast sensitivities determined for infants ($n = 47$) and adults tested at 4.7 Hz ($n = 6$) of the present study (open circles: luminance data, open squares: chromatic data). For comparison, data from Dobkins et al. (1999) are also plotted (filled circles: luminance data, filled squares: chromatic data, curves shifted upward to facilitate comparison). See text for details.

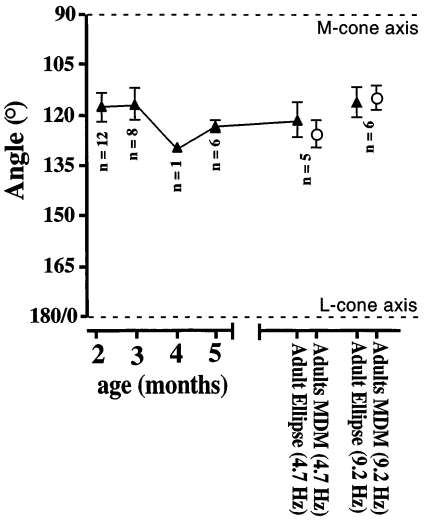

Fig. 4. Group mean angles as a function of age. Shown are the mean angles derived from the standard ellipse-fitting procedure (filled triangles). Only individuals whose data were best fit with a standard ellipse oriented in the L − M direction were included in this analysis (the number of subjects is provided below each data point). For adults, angles derived from the minimally-distinct motion (MDM) technique are also shown (open circles).

mechanisms. However, when infant data are compared to adult data, the youngest infants tested (2-month-olds of the present study) exhibited a differential loss of chromatic, with respect to luminance, sensitivity (at least for this particular spatiotemporal frequency). Specifically, the chromatic sensitivity of 2-month-olds was 1.68 log units (48-fold) worse than that of adults, whereas luminance sensitivity was only 1.46 log units (29-fold) worse. Thus, these data can be interpreted as reflecting an early retarded development of chromatic mechanisms, which then catches up to luminance mechanisms around 5 months of age. In fact, the reversed sensitivity of 4-month-olds suggests that development of mechanisms underlying chromatic sensitivity may temporarily surpass those underlying luminance sensitivity, an issue we return to in Section 4.

3.4. Group mean angles in cone contrast space as a function of age

Shown in Fig. 4 are mean angles derived from the ellipse-fitting procedure (filled triangles), which represent estimates of red/green isoluminance. Data are plotted separately for each age group (and see Table 1). For adults, angles derived from the minimally-distinct motion technique are also shown (open circles). Note that for this analysis, we necessarily excluded subjects whose data were best fit by the circle model (i.e. 12 out of 47 infants, and one adult tested at 4.7 Hz). Also, we excluded subjects whose ellipses were oriented in the L + M direction (i.e. eight of 47 infants). Our reason for excluding these data is based on the fact that these ellipses tend to be constrained to a 45° angle (since this stimulus uniquely defines the L + M direction), with the result that the axis oriented along the L − M direction (i.e. the minor, orthogonal axis of the ellipse) is constrained to 135°.

For adult data there was a close correspondence between the angles derived from the standard ellipse-fitting procedure and the minimally-distinct motion technique, indicating that the angle of the ellipse provides a reliable estimate of the individual's actual isoluminance point (and see Fig. 1a). The correlations (r) between the two measures were 0.82 and 0.87 for 4.7 Hz and 9.2 Hz conditions, respectively. In addition, for adult angles derived from both the ellipse-fitting procedure and the minimally-distinct motion technique, values were closer to 90° (i.e. the M-cone axis) for 9.2 Hz, as compared to 4.7 Hz, data. This indicates a relatively greater sensitivity to red at higher temporal frequencies, in accordance with previous studies (e.g. Cavanagh, MacLeod, & Anstis, 1987; Dobkins & Albright, 1993; Dobkins, Gunther, & Peterzell, 2000). On average, the mean angles for 4.7 Hz data were 117.5°, 116.9°, 123.5° and 121.3° for 2-, 3-, 5-month-olds and adults, respectively (the one 4-month-old in this analysis had an angle of 129.6°). Statistical analyses of these data revealed no significant difference across ages ($F(4,27) = 0.497$, P = NS). Thus, these results add to the mounting evidence for similar isoluminance points between infants and adults.

3.5. Evidence for independent chromatic and luminance mechanisms

In addition to demonstrating similar angles across ages, the data in Fig. 4 also demonstrate that the ellipses are oriented significantly away from both the L-cone isolating axis and the M-cone isolating axis ($P < 0.005$ at all ages). This suggests that, on average, infant thresholds are not limited simply by the amount of contrast in L- and M-cones. Rather, such findings suggest the existence of independent post-receptoral chromatic and luminance mechanisms.

In order to investigate this issue for individual subjects, we performed an analysis similar to that of Kelly and Chang (2000). For each data set, we determined whether our standard ellipse fit (in which the angle was allowed to vary freely) was significantly better than a fixed-angle ellipse fit that forced the angle to be within ± 4° of one of the two cone axes (see Section 2). As for data sets best fit by a circle, an ellipse oriented along the cone axes is consistent with summation between L- and M-cones (which we refer to as the 'cone summation' model). To determine which model better described the data, the fitted contour for each subject was accepted as consistent with independent mechanisms

only when the residual error in the standard ellipse model was significantly less than that from the cone summation model (see Kelly & Chang (2000) for details).

The results of these analyses are presented in Table 1. For each subject, the best-fitting parameters are shown for both the standard ellipse model (left) and cone summation model (right), with the last column indicating the statistical significance of the *F*-test between the two (see Section 2). If the last column indicates 'yes', the data were found to be significantly better fit by a model assuming independent mechanisms. For adults, all but one subject tested at 4.7 Hz (i.e. the subject whose data had been better fit by the circle model in our original analysis) yielded data that rejected the cone summation model in favor of independent chromatic and luminance mechanisms. Such findings are expected based on previous studies, which have demonstrated independent chromatic and luminance mechanisms in adults, employing techniques such as adaptation (e.g. Krauskopf, Williams, & Heeley, 1982; Bradley, Switkes, & De Valois, 1988), masking (e.g. Gegenfurtner & Kiper, 1992; Mullen & Losada, 1994; Sankeralli & Mullen, 1997; Giulianini & Eskew, 1998; Mullen & Losada, 1999), summation (e.g. Cole, Stromeyer, & Kronauer, 1990; Chaparro, Stromeyer, Kronauer, & Eskew, 1994; Mullen, Cropper, & Losada, 1997; Mullen & Sankeralli, 1999) and factor analysis (Dobkins et al., 2000; Peterzell & Teller, 2000) paradigms.

For infants, the 11 subjects who had originally been best fit by the circle model were, as expected, best fit by the cone summation model (Table 1, bold, italicized cells). In addition, another nine infants whose data originally rejected the circle model in favor of the standard ellipse model (six 2-month-olds, one 3-month-old, and two 5-month-olds) were also best fit by the cone summation model (Table 1, italicized cells). Thus, these nine infants exhibited elongated ellipses, yet the angle of the ellipse could not be distinguished from the cone axes. Interestingly, the majority of these cases (6/9) were observed in 2-month-olds. This may result, in part, from the fact that data from this age group tended to be more noisy than data from the other age groups (see MS error in Table 1). Data from the remaining 25 infants (53%) yielded data that statistically rejected the cone summation model. These results thus parallel the VEP findings of Kelly and Chang (2000), in that roughly half of our infants provided data consistent with independent chromatic and luminance mechanisms. Although this may reflect genuine differences in underlying mechanisms across infants, given the relatively low number of thresholds and the general noisiness of infant data, it is equally likely that these differences arise because some infant data sets are simply noisier than others.

4. Discussion

The results of these experiments are discussed in several contexts. First, we compare our findings to those of the steady-state VEP study of Kelly and Chang (2000), which similarly fitted infant ellipses in L- and M-cone contrast space. Second, we present the results of a simulation analysis we conducted in order to obtain estimates of error in the angle, length and width parameters in our ellipse-fitting procedure. Third, we discuss the relative development of chromatic versus luminance contrast sensitivity and speculate on possible underlying neural mechanisms, with a particular focus on magnocellular and parvocellular processing streams of the primate visual system.

4.1. Infant ellipses in L- and M-cone contrast space

The design of the present psychophysical study mirrors that of a recent visually evoked potentials (VEP) study by Kelly and Chang (2000), which employed the sweep-contrast VEP technique to obtain thresholds in infants (3.5–8 months of age) and adults. Like the present study, they fitted contours to threshold data plotted in L- and M-cone contrast space. However, in their study they tested several different contour shapes, and found that threshold data were generally best fit by an ellipse shape (i.e. where $e = 1.0$, see Eq. (2) in Section 2) rather than by more complex detection contours (e.g. a parallelogram). It was this result, in part, that led us in the present study to employ ellipses. As in the present study, Kelly and Chang investigated the existence of independent chromatic and luminance mechanisms in infants by determining whether a model based on simple cone summation (i.e. a contour oriented within $\pm 4°$ of the cone isolating axes) could better account for the data than an independent mechanisms model (i.e. that allowed the angle of the contour to vary freely). While all three of their adult data sets were best fit by the independent mechanisms model, only seven out of 13 infant data sets (54%) had a statistically better fit with the independent mechanisms model.

In addition, Kelly and Chang (2000) reanalyzed the data from two previous VEP studies (Allen et al., 1993; Morrone et al., 1993) and found similar results. That is, only half of the infants in each of these studies yielded contours in L- and M-cone contrast space that were consistent with independent mechanisms for chromatic and luminance contrast. Thus, the results from all three VEP studies are in accordance with the findings of the present psychophysical study (where 25 of 47 infants, 53%, were consistent with independence), in that all yield mixed results regarding independent mechanisms in infants. One interpretation of these findings is that only a proportion of infants (approximately half) actu-

ally possess independent chromatic and luminance mechanisms, while the others use a single mechanism for the detection of chromatic and luminance contrast. That infants may, in fact, possess a single mechanism for the detection of both types of contrast has been suggested in several previous studies, including those measuring motion:detection threshold ratios (Dobkins & Teller, 1996a; Lia, Dobkins, Palmer, & Teller, 1999), temporal contrast sensitivity functions (Dobkins et al., 1997, 1999) and in studies using factor analysis (Peterzell, Chang, & Teller, 2000; Peterzell & Teller, 2000). Alternatively, it is possible (and quite likely) that variation across infants arises from statistical noise associated with fitting ellipses that are based on relatively few threshold estimates. Had we been able to obtain more data from each infant, we suspect that a greater number of data sets would have been statistically distinguishable from the cone summation model. We would point out, however, that if infant ellipses undergo a transition from orientation in the L − M direction to orientation in the L + M direction (as the data from 4-month-olds suggest), we might expect to find that some data sets are truly best approximated by a circle.

4.2. Estimates of error in infant ellipse parameters

In our contour-fitting procedure, the degree of error in the parameter fits will depend on the reliability of the threshold estimates. Although we did not obtain estimates of threshold reliability in the present study, previous threshold studies have estimated infant test/re-test reliability to be approximately 0.3 log units (Kelly & Chang (2000) and see Teller, Mar, & Preston (1992) for similar values obtained for acuity measurements). In order to estimate the error in the parameter fits of the present experiment, we employed a computer program that simulated the effects of threshold errors on the order of ± 0.3 log units. Specifically, we took six values from a true ellipse plotted in cone contrast space (spaced in intervals of 30°), and randomly added a variation of ± 0.3 log units to each value. The new simulated values were then subjected to our ellipse-fitting procedure, and the length, width and angle parameters were determined. This was performed 60 times, in order to obtain estimates of S.D.

Three different length/width ratios were tested, one reflecting the mean across the infant subjects of the present study whose data were best fit with the standard ellipse (i.e. 2.58), one reflecting the maximum value observed across the data set (i.e. 4.92), and one reflecting the minimum value observed across the data set (i.e. 1.24). With regard to the angle parameter, the S.D. was determined to be $\pm 24.7°$ for the 'mean' ellipse. The error was substantially lower (S.D. $\pm 7.6°$) for the 'maximum' ellipse and higher (S.D. $\pm 49.6°$) for the 'minimum' ellipse. With regard to the length parameter, S.D.s were ± 0.20, 0.17, and 0.11 log units for the 'mean', 'maximum' and 'minimum' ellipse, respectively. For the width parameter, S.D.s were substantially lower, i.e. S.D.s were ± 0.11, 0.09, 0.10 log units for the 'mean', 'maximum' and 'minimum' ellipse, respectively. (We also conducted this simulation on ellipse data from infant subjects who exhibited length/width ratios at the mean, maximum and minimum values, and obtained nearly identical S.D. values.)

In sum, the results of these analyses suggest that the parameter fits for any given individual should be viewed with some caution (e.g. the error in the angle parameter for the average subject is $\pm 24.7°$), and that differences observed across infant subjects may (to some degree) reflect errors in the ellipse-fitting procedure due to noisy threshold estimates. Nonetheless, group mean infant values (such as those plotted in Figs. 3 and 4) are expected to be relatively reliable since individual subject error should cancel out when data are averaged in this fashion.

4.3. Development of chromatic versus luminance sensitivity

The results of our ellipse-fitting procedure allow us to investigate the relative development of chromatic and luminance contrast sensitivity. Although this topic has been addressed by many previous psychophysical and VEP studies (e.g. Allen et al., 1993; Morrone et al., 1993; Teller & Lindsey, 1993; Brown et al., 1995; Dobkins & Teller, 1996a; Teller & Palmer, 1996; Dobkins et al., 1997; Kelly et al., 1997; Crognale et al., 1998; Dobkins et al., 1999), the present study is unique in that the ellipse-fitting procedure can help yield more precise estimates of chromatic (red/green) sensitivity. This is because previous studies have typically used a single, nominally-isoluminant red/green stimulus for all infants (e.g. based on the mean isoluminance point of adult subjects). Given known variability in isoluminance points across individuals, this method necessarily results in a proportion of subjects being tested with red/green stimuli that contain residual luminance contrast, which, in turn, is expected to yield an overestimation of infants' chromatic sensitivity. The advantage of the ellipse-fitting procedure is that infants need not be tested with perfectly isoluminant stimuli. Instead, individual isoluminance and chromatic thresholds are parameters of the ellipse fit, which is based on several threshold estimates. It is important to point out, however, that the accuracy of these parameters will depend on the reliability of the infant thresholds that make up the ellipse. As described above (Section 4.2), the error can be substantial in some cases. Thus, we acknowledge that although, in theory, the ellipse fit should yield greater accuracy, this may not be true in practice in all cases.

When we plot chromatic and luminance sensitivities derived from the ellipse-fitting procedure (Fig. 3), we find a steeper increase in chromatic, with respect to luminance, sensitivity between 2 and 5 months of age. At 2 months of age, infants exhibit a differential loss of chromatic, with respect to luminance, sensitivity (i.e. their performance differs from adults more for chromatic than for luminance stimuli), a result which mirrors that reported in VEP studies (Morrone, Burr, & Fiorentini, 1990; Morrone et al., 1993; Kelly et al., 1997; Crognale et al., 1998). This finding indicates a relatively retarded development of mechanisms underlying chromatic sensitivity in the first couple of months (at least for the spatiotemporal frequencies used in these experiments). At 4 months of age, however, infants become more sensitive to chromatic than to luminance contrast, a pattern which is opposite to that observed at all other ages (including adults). This surprising result, which now replicates that observed in our previous study (see Dobkins et al. (1999)), suggests that the development of chromatic mechanisms may catch up and even surpass the development of luminance mechanisms for a brief period in time.

4.4. Possible underlying neural mechanisms

In order to elucidate potential neural substrates underlying these results, we turn to the known response properties of neurons in the macaque visual system. Comparisons between macaques and humans are justified based on the known similarities between the visual systems of the two primates (e.g. De Valois, Morgan, & Snodderly, 1974a, b). In particular, we focus on the properties of two distinct subcortical pathways — parvocellular and magnocellular — which originate in the retina and remain segregated up through layer 4C of area V1 (see Merigan and Maunsell (1993) for review). (Note that there also exists a third pathway, the 'koniocellular' pathway, which originates in the blue-ON bistratified cells of the retina. These cells receive $S-(L+M)$ cone input and are thought to encode 'blue/yellow' chromatic information (see Hendry and Reid (2000)). Although an $S-(L+M)$ mechanism can be expected to respond to luminance stimuli, by virtue of its $L+M$ input, it is generally accepted (in the adult literature) that the sensitivity of this mechanism to luminance stimuli is far inferior to that of the $L+M$ mechanism, and thus the $S-(L+M)$ mechanism is thought not to contribute to luminance thresholds revealed psychophysically (e.g. Ruttiger & Lee, 2000). Although we cannot rule out the possibility for $S-(L+M)$ contribution in infants, we feel this possibility highly unlikely since the $S-(L+M)$ mechanism it thought to be particularly slow to develop in infants (e.g. Varner, Cook, Schneck, McDonald, & Teller, 1985; Banks & Bennett, 1988). For this reason, we do not discuss the contribution of the $S-(L+M)$, i.e. koniocellular, pathway further here.)

Neurophysiological studies investigating the response properties of parvocellular and magnocellular cells (in the retina and lateral geniculate nucleus) of adult macaques have demonstrated marked differences in the relative sensitivities of these two cell types to chromatic (red/green) and luminance contrast. Specifically, magnocellular cells are far more sensitive to luminance contrast than are parvocellular cells, whereas parvocellular cells are far more sensitive to chromatic contrast than are magnocellular cells (e.g. Hicks, Lee, & Vidyasagar, 1983; Derrington & Lennie, 1984; Lee, Pokorny, Smith, Martin, & Valberg, 1990). Based on these differences, the claim has often been made that magnocellular and parvocellular pathways provide the neural substrate for luminance and chromatic contrast sensitivity, respectively (e.g. Lee et al., 1990; Smith, Pokorny, Davis, & Yeh, 1995; Dobkins et al., 1999). This segregation of function is also thought to explain the above-described results from adult psychophysical studies demonstrating independent mechanisms for chromatic and luminance contrast (but see Ingling & Martinez-Uriegas (1983), Lennie & D'Zmura (1988), De Valois & De Valois (1993), Billock (1995), Mullen et al. (1997) for arguments that the parvocellular pathway may subserve both types of contrast sensitivity).

In infants, it is unknown whether luminance and chromatic contrast sensitivity are governed by magnocellular and parvocellular pathways, respectively, since the response properties of these pathways have yet to be thoroughly explored in infant macaques. If, like adults, infant magnocellular and parvocellular cells underlie luminance and chromatic sensitivity, respectively, the results of the present study suggest that the differential loss in chromatic, with respect to luminance, sensitivity observed in 2-month-olds reflects relatively faster development for the magnocellular pathway at least within the first 2 months (and see Dobkins & Teller (1996a), Dobkins et al. (1999)). In fact, this possibility of faster magnocellular, with respect to parvocellular, pathway development is generally supported by studies of anatomical growth and synapse formation in infant primates (macaques: Mates & Lund, 1983; Lund & Harper, 1991; Lund & Holbach, 1991; Distler, Bachevalier, Kennedy, Mishkin, & Ungerleider, 1996, but cf. Chalupa, Meissirel, & Lia, 1996 for embryonic data; galagos: Lachica & Casagrande, 1988; Florence & Casagrande, 1990; humans: Burkhalter, Bernardo, & Charles, 1993, but cf. Hickey, 1977 and see Movshon, Kiorpes, Hawken, Skoczenski, Cavanaugh, & Graham, 1997 for neurophysiological experiments demonstrating faster development of temporal resolution in magnocellular cells of macaques as compared to parvocellular cells).

In a similar vein, we propose that results from 4-month-olds of the present study suggest a significant acceleration in parvocellular cell development, since at this age infants exhibit a differential loss for luminance contrast. By 5 months of age the pattern changes to a uniform loss of sensitivity (i.e. the performance of 5-month-olds differs from adults equally for chromatic (11.7-fold) and luminance (12.0-fold) stimuli). In total, these results suggest that the relative developmental rate of magnocellular and parvocellular pathways may change dynamically during the first 3–5 months of age, but then stabilize at around 5 months. Without data from older infants, however, we cannot rule out the possibility that further changes in the relative rates occur after this point. In fact, results from recent electrophysiological (e.g. Crognale et al. 1998) and behavioral (e.g. Hollants-Gilhuijs, Ruijter, & Spekreijse, 1998; Knoblauch, Vital-Durand, & Barbur, 2001) studies suggest that chromatic mechanisms continue to mature relative to luminance mechanisms long after 5 months of age and perhaps even into puberty. In any event, the results from the present study predict that neural immaturities in the processing of chromatic and luminance stimuli will be found in neurophysiological explorations of magnocellular and parvocellular cells in infant primates.

Acknowledgements

This work was supported by NIH grant EY12153 (KRD). We thank S. Apgar, J. Connellan, D. Romann and E. Wang (undergraduates at UC San Diego) for assistance with infant data collection.

References

Allen, D., Banks, M. S., & Norcia, A. M. (1993). Does chromatic sensitivity develop more slowly than luminance sensitivity? *Vision Research*, *33*, 2553–2562.

Anderson, C. M., & Dobkins, K. R. (1999). Do infants sum sub-threshold levels of luminance and chromatic contrast?: Evidence from 2, 3, 4, and 5-month-olds. *Investigative Ophthalmology and Visual Science (Supplement)*, *40*, S395.

Atkinson, J., Braddick, O., & Moar, K. (1977). Contrast sensitivity of the human infant for moving and static patterns. *Vision Research*, *17*, 1045–1047.

Banks, M. S., & Bennett, P. J. (1988). Optical and photoreceptor immaturities limit the spatial and chromatic vision of human neonates. *Journal of the Optical Society of America A*, *5*, 2059–2079.

Banks, M. S., & Salapatek, P. (1978). Acuity and contrast sensitivity in 1-, 2-, and 3-month-old human infants. *Investigative Ophthalmology and Visual Science*, *17*, 361–365.

Bieber, M. L., Kraft, J. M., & Werner, J. S. (1998). Effects of known variations in photopigments on L/M cone ratios estimated from luminous efficiency functions. *Vision Research*, *38*, 1961–1966.

Bieber, M. L., Volbrecht, V. J., & Werner, J. S. (1995). Spectral efficiency measured by heterochromatic flicker photometry is similar in human infants and adults. *Vision Research*, *35*, 1385–1392.

Billock, V. A. (1995). Cortical simple cells can extract achromatic information from the multiplexed chromatic and achromatic signals in the parvocellular pathway. *Vision Research*, *35*, 2359–2369.

Bradley, A., Switkes, E., & De Valois, K. (1988). Orientation and spatial frequency selectivity of adaptation to color and luminance gratings. *Vision Research*, *28*, 841–856.

Brown, A. M., Lindsey, D. T., McSweeney, E. M., & Walters, M. M. (1995). Infant luminance and chromatic contrast sensitivity: optokinetic nystagmus data on 3-month-olds. *Vision Research*, *35*, 3145–3160.

Burkhalter, A., Bernardo, K. L., & Charles, V. (1993). Development of local circuits in human visual cortex. *Journal of Neuroscience*, *13*, 1916–1931.

Cavanagh, P., & Anstis, S. (1991). The contribution of color to motion in normal and color-deficient observers. *Vision Research*, *31*, 2109–2148.

Cavanagh, P., MacLeod, D. I., & Anstis, S. M. (1987). Equiluminance: spatial and temporal factors and the contribution of blue-sensitive cones. *Journal of the Optical Society of America A*, *4*, 1428–1438.

Chalupa, L. M., Meissirel, C., & Lia, B. (1996). Specificity of retinal ganglion cell projections in the embryonic rhesus monkey. *Perspectives on Developmental Neurobiology*, *3*, 223–231.

Chaparro, A., Stromeyer, C. F. I., Huang, E. P., Kronauer, R. E., & Eskew, R. T. J. (1993). Colour is what the eye sees best. *Nature*, *361*, 348–350.

Chaparro, A., Stromeyer, C. F. I., Kronauer, R. E., & Eskew, R. T. J. (1994). Separable red–green and luminance detectors for small flashes. *Vision Research*, *34*, 751–762.

Chien, S. H., Teller, D. Y., & Palmer, J. (2000). The transition from scotopic to photopic vision in 3-month-old infants and adults: an evaluation of the rod dominance hypothesis. *Vision Research*, *40*, 3853–3872.

Cole, G. R., Hine, T., & McIlhagga, W. (1993). Detection mechanisms in L-, M-, and S-cone contrast space. *Journal of the Optical Society of America A*, *10*, 38–51.

Cole, G. R., Stromeyer, C. F. I., & Kronauer, R. E. (1990). Visual interactions with luminance and chromatic stimuli. *Journal of the Optical Society of America A*, *7*, 128–140.

Cowan, C. B. (1983). An inexpensive scheme for calibration of a colour monitor in terms of CIE standard coordinates. *Computer Graphics*, *17*, 315–321.

Crognale, M. A., Kelly, J. P., Weiss, A. H., & Teller, D. Y. (1998). Development of the spatio-chromatic visual evoked potential (VEP): a longitudinal study. *Vision Research*, *38*, 3283–3292.

Crone, R. A. (1959). Spectral sensitivity in color-defective subjects and heterozygous carriers. *American Journal of Ophthalmology*, *48*, 231–238.

De Valois, R. L., & De Valois, K. K. (1993). A multi-stage color model. *Vision Research*, *33*, 1053–1065.

De Valois, R. L., Morgan, H., & Snodderly, D. M. (1974a). Psychophysical studies of monkey vision. 3. Spatial luminance contrast sensitivity tests of macaque and human observers. *Vision Research*, *14*, 75–81.

De Valois, R. L., Morgan, H. C., Polson, M. C., Mead, W. R., & Hull, E. M. (1974b). Psychophysical studies of monkey vision. I. Macaque luminosity and color vision tests. *Vision Research*, *14*, 53–67.

Derrington, A. M., & Lennie, P. (1984). Spatial and temporal contrast sensitivities of neurones in lateral geniculate nucleus of macaque. *Journal of Physiology (London)*, *357*, 219–240.

Distler, C., Bachevalier, J., Kennedy, C., Mishkin, M., & Ungerleider, L. G. (1996). Functional development of the corticocortical

pathway for motion analysis in the macaque monkey: a 14C-2-deoxyglucose study. *Cerebral Cortex*, *6*, 184–195.

Dobkins, K. R., & Albright, T. D. (1993). What happens if it changes color when it moves?: Psychophysical experiments on the nature of chromatic input to motion detectors. *Vision Research*, *33*, 1019–1036.

Dobkins, K. R., & Teller, D. Y. (1996a). Infant motion:detection (M:D) ratios for chromatic-defined and luminance-defined moving stimuli. *Vision Research*, *36*, 3293–3310.

Dobkins, K. R., & Teller, D. Y. (1996b). Infant contrast detectors are selective for direction of motion. *Vision Research*, *36*, 281–294.

Dobkins, K. R., Anderson, C. M., & Lia, B. (1999). Infant temporal contrast sensitivity functions (tCSFs) mature earlier for luminance than for chromatic stimuli: evidence for precocious magnocellular development? *Vision Research*, *39*, 3223–3239.

Dobkins, K. R., Gunther, K. L., & Peterzell, D. H. (2000). What covariance mechanisms underlie green/red equiluminance, chromatic contrast sensitivity and luminance contrast sensitivity? *Vision Research*, *40*, 613–628.

Dobkins, K. R., Lia, B., & Teller, D. Y. (1997). Infant color vision: temporal contrast sensitivity functions (tCSFs) for chromatic (red/green) stimuli in 3-month-olds. *Vision Research*, *37*, 2699–2716.

Flitcroft, D. I. (1989). The interactions between chromatic aberration, defocus and stimulus chromaticity: implications for visual physiology and colorimetry. *Vision Research*, *29*, 349–360.

Florence, S. L., & Casagrande, V. A. (1990). Development of geniculocortical axon arbors in a primate. *Visual Neuroscience*, *5*, 291–309.

Gegenfurtner, K. R., & Hawken, M. J. (1995). Temporal and chromatic properties of motion mechanisms. *Vision Research*, *35*, 1547–1563.

Gegenfurtner, K. R., & Kiper, D. C. (1992). Contrast detection in luminance and chromatic noise. *Journal of the Optical Society of America A*, *9*, 1880–1888.

Giulianini, F., & Eskew, R. T. J. (1998). Chromatic masking in the (L/L, M/M) plane of cone-contrast space reveals only two detection mechanisms. *Vision Research*, *38*, 3913–3926.

Hartmann, E. E., & Banks, M. S. (1992). Temporal contrast sensitivity in human infants. *Vision Research*, *32*, 1163–1168.

Hendry, S. H. C., & Reid, R. C. (2000). The koniocellular pathway in primate vision. *Annual Review of Neuroscience*, *23*, 127–153.

Hickey, T. L. (1977). Postnatal development of the human lateral geniculate nucleus: relationship to a critical period for the visual system. *Science*, *198*, 836–838.

Hicks, T. P., Lee, B. B., & Vidyasagar, T. R. (1983). The responses of cells in macaque lateral geniculate nucleus to sinusoidal gratings. *Journal of Physiology (London)*, *337*, 183–200.

Hollants-Gilhuijs, M. A., Ruijter, J. M., & Spekreijse, H. (1998). Visual half-field development in children: detection of colour-contrast-defined forms. *Vision Research*, *38*, 645–649.

Ingling, C. R., & Martinez-Uriegas, E. (1983). The relationship between spectral sensitivity and spatial sensitivity for the primate R ∧ g X-channel. *Vision Research*, *23*, 1495–1500.

Kelly, J. P., & Chang, S. (2000). Development of chromatic and luminance detection contours using the sweep VEP. *Vision Research*, *40*, 1887–1906.

Kelly, J. P., Borchert, K., & Teller, D. Y. (1997). The development of chromatic and achromatic contrast sensitivity in infancy as tested with the sweep VEP. *Vision Research*, *37*, 2057–2072.

Knoblauch, K., & Maloney, L. T. (1996). Testing the indeterminacy of linear color mechanisms from color discrimination data. *Vision Research*, *36*, 295–306.

Knoblauch, K., Vital-Durand, F., & Barbur, J. L. (2001). Variation of chromatic sensitivity across the life span. *Vision Research*, *40*, 22–36.

Krauskopf, J., Williams, D. R., & Heeley, D. W. (1982). Cardinal directions of color space. *Vision Research*, *22*, 1123–1131.

Lachica, E. A., & Casagrande, V. A. (1988). Development of primate retinogeniculate axon arbors. *Visual Neuroscience*, *1*, 103–123.

Lee, B. B., Pokorny, J., Smith, V. C., Martin, P. R., & Valberg, A. (1990). Luminance and chromatic modulation sensitivity of macaque ganglion cells and human observers. *Journal of the Optical Society of America A*, *7*, 2223–2236.

Lennie, P., & D'Zmura, M. (1988). Mechanisms of color vision. *Critical Reviews in Neurobiology*, *3*, 333–400.

Lia, B., Dobkins, K. D., Palmer, J., & Teller, D. Y. (1999). Infants code the direction of chromatic quadrature motion. *Vision Research*, *39*, 1783–1794.

Lund, J. S., & Harper, T. R. (1991). Postnatal development of thalamic recipient neurons in the monkey striate cortex: III. Somatic inhibitory synapse acquisition by spiny stellate neurons of layer 4C. *Journal of Comparative Neurolology*, *309*, 141–149.

Lund, J. S., & Holbach, S. M. (1991). Postnatal development of thalamic recipient neurons in the monkey striate cortex: I. Comparison of spine acquisition and dendritic growth of layer 4C alpha and beta spiny stellate neurons. *Journal of Comparative Neurology*, *309*, 115–128.

MacLeod, D. I., & Boynton, R. M. (1979). Chromaticity diagram showing cone excitation by stimuli of equal luminance. *Journal of the Optical Society of America*, *69*, 1183–1186.

Mates, S. L., & Lund, J. S. (1983). Developmental changes in the relationship between type 2 synapses and spiny neurons in the monkey visual cortex. *Journal of Comparative Neurolology*, *221*, 98–105.

Maurer, D., Lewis, T. L., Cavanagh, P., & Anstis, S. (1989). A new test of luminous efficiency for babies. *Investigative Ophthalmology and Visual Science*, *30*, 297–303.

Merigan, W. H., & Maunsell, J. H. (1993). How parallel are the primate visual pathways? *Annual Review of Neuroscience*, *16*, 369–402.

Morrone, M. C., Burr, D. C., & Fiorentini, A. (1990). Development of contrast sensitivity and acuity of the infant colour system. *Proceedings of the Royal Society of London B Biological Sciences*, *242*, 134–139.

Morrone, M. C., Burr, D. C., & Fiorentini, A. (1993). Development of infant contrast sensitivity to chromatic stimuli. *Vision Research*, *33*, 2535–2552.

Movshon, J. A., Kiorpes, L., Hawken, M. J., Skoczenski, A. M., Cavanaugh, J. R., & Graham, N. V. (1997). Sensitivity of LGN neurons in infant macaque monkey. *Investigative Ophthalmology and Visual Science (Supplement)*, *15*(38), S498.

Mullen, K. T., & Losada, M. A. (1994). Evidence for separate pathways for color and luminance detection mechanisms. *Journal of the Optical Society of America A*, *11*, 3136–3151.

Mullen, K. T., & Losada, M. A. (1999). The spatial tuning of color and luminance peripheral vision measured with notch filtered noise masking. *Vision Research*, *39*, 721–732.

Mullen, K. T., & Sankeralli, M. J. (1999). Evidence for the stochastic independence of the blue–yellow, red–green and luminance detection mechanisms revealed by subthreshold summation. *Vision Research*, *39*, 733–745.

Mullen, K. T., Cropper, S. J., & Losada, M. A. (1997). Absence of linear subthreshold summation between red–green and luminance mechanisms over a wide range of spatio-temporal conditions. *Vision Research*, *37*, 1157–1165.

Noorlander, C., Heuts, M. J., & Koenderink, J. J. (1981). Sensitivity to spatiotemporal combined luminance and chromaticity contrast. *Journal of the Optical Society of America*, *71*, 453–459.

Peterzell, D. H., & Teller, D. Y. (2000). Spatial frequency tuned covariance channels for red–green and luminance-modulated gratings: psychophysical data from human adults. *Vision Research*, *40*, 417–430.

Peterzell, D. H., Chang, S. K., & Teller, D. Y. (2000). Spatial frequency tuned covariance channels for red–green and lumi-

nance-modulated gratings: psychophysical data from human infants. *Vision Research*, *40*, 431–444.

Poirson, A. B., Wandell, B. A., Varner, D. C., & Brainard, D. H. (1990). Surface characterizations of color thresholds. *Journal of the Optical Society of America A*, *7*, 783–789.

Rasengane, T. A., Allen, D., & Manny, R. E. (1997). Development of temporal contrast sensitivity in human infants. *Vision Research*, *37*, 1747–1754.

Ruttiger, L., & Lee, B. B. (2000). Chromatic and luminance contributions to a hyperacuity task. *Vision Research*, *40*, 817–832.

Sankeralli, M. J., & Mullen, K. T. (1996). Estimation of the L-, M-, and S-cone weights of the postreceptoral detection mechanisms. *Journal of the Optical Society of America A*, *13*, 906–915.

Sankeralli, M. J., & Mullen, K. T. (1997). Postreceptoral chromatic detection mechanisms revealed by noise masking in three-dimensional cone contrast space. *Journal of the Optical Society of America*, *14*, 2633–2646.

Smith, V. C., Pokorny, J., Davis, M., & Yeh, T. (1995). Mechanisms subserving temporal modulation sensitivity in silent-cone substitution. *Journal of the Optical Society of America A*, *12*, 241–249.

Stockman, A., MacLeod, D. I., & Johnson, N. E. (1993). Spectral sensitivities of the human cones. *Journal of the Optical Society of America A*, *10*, 2491–2521.

Stromeyer, C. F. I., Cole, G. R., & Kronauer, R. E. (1985). Second-site adaptation in the red–green chromatic pathways. *Vision Research*, *25*, 219–237.

Swanson, W. H. (1991). Heterochromatic modulation photometry in heterozygous carriers of congenital color defects. In B. Drums, J. D. Moreland, & A. Serra, *Colour vision deficiencies* (pp. 457–471). Dordrecht: Kluwer.

Teller, D. Y. (1979). The forced-choice preferential looking procedure: a psychophysical technique for use with human infants. *Infant Behavior and Development*, *2*, 135–153.

Teller, D. Y., & Lindsey, D. T. (1989). Motion nulls for white versus isochromatic gratings in infants and adults. *Journal of the Optical Society of America A*, *6*, 1945–1954.

Teller, D. Y., & Lindsey, D. T. (1993). Infant color vision: OKN techniques and null plane analysis. In K. Simons, *Infant vision: basic and clinical research*. New York: Oxford university Press.

Teller, D. Y., & Palmer, J. (1996). Infant color vision: motion nulls for red/green vs luminance-modulated stimuli in infants and adults. *Vision Research*, *36*, 955–974.

Teller, D. Y., Mar, C., & Preston, K. L. (1992). Statistical properties of 500-trial infant psychometric functions. In L. A. Werner, & E. W. Rubel, *Developmental psychoacoustics* (pp. 211–227). Washington DC: American Psychological Association.

Teller, D. Y., Pereverzeva, S., Chien, H., & Palmer, J. (2000). Are infant and adult luminance matches the same? *Investigative Ophthalmology and Visual Science (Supplement)*, *41*, S727.

Varner, D., Cook, J. E., Schneck, M. E., McDonald, M. A., & Teller, D. Y. (1985). Tritan discriminations by 1- and 2-month-old human infants. *Vision Research*, *25*, 821–831.